ACS OMEGA

Open Access

http://pubs.acs.org/journal/acsodf

Article

Uptake and Release Kinetics Longevity in Stimuli-Responsive Hydrogels for Hydrophilic Drug Therapy

Parker M. Toews and Jeffrey S. Bates*

Cite This: *ACS Omega* 2025, 10, 4580−4587

Read Online

ACCESS | Metrics & More | Article Recommendations

ABSTRACT: The uptake and release of target molecules were studied in hydrogels as a function of time over a month to determine what, if any, deviation exists in these properties. Through the use of spectroscopic techniques such as FT-IR and UV−vis−NIR in combination with drug release kinetics and swelling kinetics studies, both the effect of imprinting and the effect of time could be substantially analyzed for hydrogels. Molecular imprinting provides a significant advantage over nonimprinted hydrogel samples through the sustainment of a first-order release profile throughout the month without significant deviations in the releasable concentration, while nonimprinted samples struggle in their capability to be consistently load-cycled. Changes between the imprinted and nonimprinted samples are not evidenced to be significant chemical deviations; rather, they are attributable to functionality differences between the release mechanisms of these hydrogels.

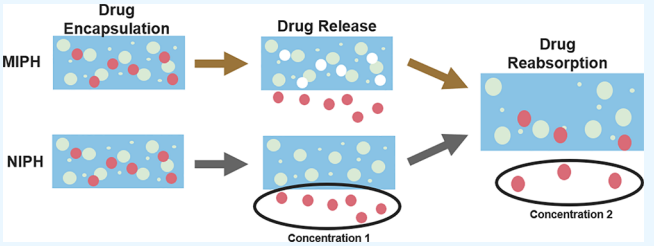

1. INTRODUCTION

Ophthalmic conditions including glaucoma, dry eye, and conjunctivitis present impacts on vast populations of individuals with 80 million, 345 million, and 100 million people, respectively, being impacted by these conditions.[1−4] Left untreated, these can lead to vision impairment and furthermore, vision loss.[5] Typically, eye-drop medications are prescribed for the treatment of these diseases which use either a lubricating nature or containment of a beta-blocker or antihistamine.[6] Eye drops, though a viable treatment solution, are not without their flaws, which include a heavy reliance on the patient themselves to effectively administer the medication at minimum once daily. The improper administration of the drug may lead to spillage which requires further alterations in dosages to treat the ocular condition at hand.[7−9] Furthermore, the use of eye drops can spark anxiety and fear in individuals and lead to less-than-desirable side effects including irritation from preservatives in the eye drops, poor taste due to drainage through nasal ducts, and temporary blurry vision after application of the medication.[10] Given that globally there are over 125 million contact lens wearers whereby contact lenses are predominantly composed of hydrogel materials, there is a demonstrated viability and applicability for the use of hydrogel materials as contact lens-based drug delivery vehicles.[11,12] Glaucoma, in particular, uses beta-blocker medications like timolol maleate which help to reduce the intraocular pressure in the eye through blocking the production of aqueous humor in the eye.[13] Typically, this requires administration at least twice daily which further propagates the potential for misadministration of the medication to occur, potentially leading to further complications in the short and long term.[14]

Hydrogels are described as biocompatible, hydrophilic, network polymers with a determinable and tunable stimuli-response. Their properties alongside their mechanical and chemical properties have made them of particular interest for use in biomedicine as sensors, actuators, tissue scaffolds, and drug delivery devices.[15−18] The structure of hydrogels is often dictated by their internal components including attached functional groups, the backbone monomer, and cross-linking monomer. Functional groups attached to the backbone chain provide chemical recognition, interatomic interactions with target molecules, and water insolubility for the hydrogel.[19,20] Alongside functional groups attached to the backbone, cross-linking of the material improves the mechanical properties and responsiveness of these materials. Cross-linking can be accomplished through two classifications, chemical and physical. Chemical cross-links are an irreversible process whereby covalent bonds are introduced into the system whereas physical cross-links are reversible, do not require a cross-linking agent, and are often described through hydrogen bonds, ionic interactions, or amphiphilic grafting.[21−23]

Received: September 17, 2024
Revised: December 12, 2024
Accepted: December 17, 2024
Published: January 29, 2025

Table 1. Mole Fraction (x_i) of the Composition Monomers[a]

	HEMA	TEGDMA	DMAEMA	EG	TEMED	APS	TM
MIPH	0.25238	0.01887	0.03222	0.68556	0.00215	0.00800	0.00803
NIPH	0.25442	0.01902	0.03248	0.69111	0.00216	0.00801	/

[a]Molecular imprinted (MIPH) contains timolol maleate with the pre-polymerized solution while the non-imprinted (NIPH) does not contain timolol maleate in the pre-polymerized solution.

Drug delivery is accomplished by leveraging the stimuli response.[24] These stimuli-responses in hydrogels are driven by structural or mechanical changes in response to environmental triggers. These structural or mechanical changes drive thermodynamic instability in the material which can be leveraged to press target molecules, such as drugs, out of the hydrogel and into the environment.[25] A wide range of stimuli-responses can be programmed into the hydrogel with pH, temperature, ions, stress, and enzymes being specific examples pertinent to biomedicine.[24−27] Demonstrations of hydrogel drug delivery vehicles have been shown to treat ocular conditions among many others by utilizing swelling or deswelling of the hydrogel to effectively excrete drug into the desired location.[28−30]

Molecular imprinting (MIP) was originally developed as a methodology to introduce high specificity and recognition of target biomolecules and foster a tunable stimuli response in hydrogel systems, namely in drug delivery systems.[31,32] This strategy of drug release leverages van der Waal interactions or hydrogen bonds between the backbone and target molecule, enhancing the retention and recognizability of the target molecule.[33] To prepare molecularly imprinted hydrogels, the target molecule is mixed into the prepolymerized solution, and as polymerization occurs, the target molecule becomes incorporated into the matrix filling voids of the hydrogel and retained through the functionalization of van der Waal interactions or hydrogen bonding as previously described.[34,35]

Studies such as Zhang et al. and Li et al. have demonstrated how these materials can facilitate the incorporation of molecules through recognition sites and how these sites can be refined through the implementation of advanced fabrication technologies such as electrospinning.[36,37] More broadly, MIP has been demonstrated as a strategy that facilitates more stable release profiles compared to nonimprinted hydrogels. These studies often address the release kinetics within a 12-h or 24-h release time frame; however, they negate the long-term applicability, so while MIP is a significant advance in the field of hydrogel drug delivery, there has not been a fundamental characterization into the longevity of drug release and more broadly, how these materials change over time.[38−41] To effectively develop these materials as a usable and dependable device, it is important to quantify the drug release kinetics and swelling kinetics as a function of time. This article in particular seeks to introduce this subject area, present some key results as a preliminary study, and pave the way for future studies into the longevity characteristics of these hydrogels, namely, mechanical and chemical.

2. MATERIALS AND METHODS

2.1. Materials. Ammonium persulfate (APS), 2-(dimethylamino) ethyl methacrylate (DMAEMA), ethylene glycol (EG), 2-hydroxyethyl methacrylate (HEMA), tetraethylene glycol dimethacrylate (TEGMDA), N,N,N′,N′-tetramethylethylenediamine (TEMED), and timolol maleate (TM) were purchased from Sigma-Aldrich (St Louis, MO, USA) and used as received for synthesis without the need for further purification. Table 1, below, demonstrates the mole fractions of each of the composite monomers within the hydrogel. The values as described were retained for all samples of either the molecular imprinted (MIPH) or nonimprinted (NIPH) variety.

Using this table, the future methods section is motivated, which describes how each of the hydrogels was fabricated for their future analysis. As can be noted, no initial drug is introduced into the nonimprinted hydrogel platform, which is addressed in the methods section of the article, specifically section 2B regarding the preparation of this classification of hydrogels.

2.2. Methods. *2.2.1. Molecularly Imprinted Hydrogel (MIPH) Preparation.* Hydrogels were produced through a thermo-initiated, free radical polymerization reaction. This process began by combining a free radical initiator (APS) and solvent (EG) and mixing these together for 10 min at room temperature or until the solid powder APS was completely absorbed into the liquid EG. Alongside the solvent-initiator formulation, the backbone (HEMA), pH-sensitive monomer (DMAEMA), cross-linker (TEGDMA), catalyst (TEMED), and target molecule (timolol) were combined in a separate test tube and mixed for 10 min at room temperature. Upon mixing, formulations were promptly placed in a refrigerator for 24 h at 5.0 °C. At the conclusion of the 24 h, both formulations were removed and combined with the backbone formulation being mixed into the solvent formulation for 10 min or until completely mixed. Once mixed, the new solution was promptly poured into a glass-slide mold and placed into a refrigerator for 24 h at 5.0 °C. At the end of this process, samples were removed from the mold and cut into 5 × 5 mm^2 samples (1.5 mm in depth from the mold) for future testing.

Schematically, the MIPH system leverages hydrogen-bonding interactions between the target molecule (timolol maleate) and the cross-linker (TEGDMA) of the hydrogel. This is demonstrated in Figure 1, found below.

As illustrated, these bonding locations in turn become recognition sites as the hydrogel is functionalized to incorporate the target molecule. Subsequently, this means that the target molecule can be removed from the matrix yet

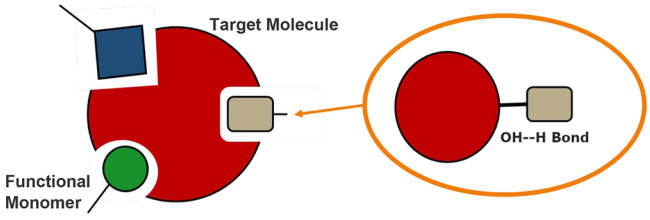

Figure 1. Demonstrating the interaction found within the molecular-imprinted (MIP) hydrogel system. Functional monomers are chemical sites where the target molecule can bind or be attached to the hydrogel. Often these are termed as recognition sites that have an affinity for the target molecule itself.

https://doi.org/10.1021/acsomega.4c08540
ACS Omega 2025, 10, 4580−4587

still retain the necessary functionality such that the drug can be reintroduced into the hydrogel matrix without affecting the hydrogel.

2.2.2. Non-Imprinted Hydrogel (NIPH) Preparation. Hydrogels were prepared through thermo-initiated, free-radical polymerization reactions. This began by combining a free radical initiator (APS) and solvent (EG) and mixing for 10 min at room temperature until the solid powder APS was completely absorbed into the liquid EG. Alongside the solvent-initiator formulation, Alongside the solvent-initiator formulation, the backbone (HEMA), pH-sensitive monomer (DMAEMA), cross-linker (TEGDMA), and catalyst (TEMED) were combined in a separate test tube and mixed for 10 min at room temperature. Formulations were then mixed for 10 min at room temperature or until completely incorporated with one another. The end solution was then promptly poured into a glass-slide mold and placed into a refrigerator for 24 h at 5.0 °C. At the end of this process, samples were removed from the mold and cut into 5 × 5 mm^2 samples (1.5 mm in depth from the mold) for future testing. Timolol was loaded into the NIPH hydrogel leveraging a 24 h soak within a solution of the same concentration as the MIPH hydrogel. This leverages the functionality of hydrogel affinity to absorb and desorb quantities of water without the development of recognition sites within the hydrogel matrix, meaning the limitation is on the void sizes of the hydrogel.

2.2.3. UV−Vis−NIR Analysis. A PerkinElmer (Waltham, MA, USA) Lambda 950 UV−vis−NIR spectrophotometer was used to collect spectroscopic data between wavelengths of 300−900 nm with a sampling step of 2 nm. The UV−vis−NIR spectrophotometer was used to determine the clarity of the synthesized hydrogels as well as for drug release experimentation through the Beer−Lambert Law. The former experiments used an Integrating Sphere (IS) attachment while the latter used a 2D Detector. Prior to data collection, the lamps were allowed to warm for one hour. If an attachment change was necessary as well, this would be conducted prior to the warm-up period. Hydrogels for UV−vis−NIR measurements were taken directly from their trimmed-down dimensions and directly measured.

2.2.4. FT-IR Analysis. A ThermoFisher Scientific (Waltham, MA, USA) Nicolet iS50 Fourier-transform infrared spectrometer (FT-IR) was utilized in the study to identify functional groups and structures present in the synthesized hydrogel samples. This FT-IR system uses attenuated total reflectance (ATR) with a KBR crystal, which allows the direct sampling of synthesized hydrogels in the solid state without the need for advanced processing or preparation. Prior to data collection, the system was allowed to warm up for one hour. No attachment changes were applicable to this instrument. Hydrogels for FT-IR measurements were taken from their trimmed-down dimensions and directly measured.

2.2.5. Swelling Kinetics Analysis. The swelling kinetics of the prepared hydrogel samples were determined by first measuring the mass of the dry hydrogel sample, M_d, and immersing them in a buffer solution with a pH of 7.4. Hydrogel samples were allowed to immerse in the buffer solution for 12 h, where a final mass would be recorded, M_s. The percentage swelling in each hydrogel sample follows eq 1,

$$\%\ \text{Swelling} = 100\left(\frac{M_s - M_d}{M_d}\right) \tag{1}$$

where M_d is the dry mass of the hydrogel samples prior to immersion in the buffer solution and M_s is the swollen mass of the hydrogel sample after the 12-h period immersed in the buffer solution. The dimensions of each hydrogel sample are the same, and thus the volume should be a constant factor, meaning no normalization between samples is required for direct comparison.

2.2.6. Drug Uptake and Release Kinetics Analysis. The drug uptake and release kinetics of the prepared hydrogel samples were determined by completely submerging dry hydrogel samples into a buffer solution with a pH of 7.4 allowing for drug release in the *x*, *y*, and *z*-directions. The drug was allowed to be released for a total of 12 h at intervals of 1 h. After the 12 h elution in the buffer solution, the hydrogel samples were then immersed into a second solution for 12 h to release the remainder of the drug within the matrix. Both solutions were characterized to determine the concentration of drug released into each solution and the percentage of total drug released at each time interval. This experiment was expanded as needed within this paper to test the longevity of the uptake and release profile over a month's time. All solutions were maintained at 1000 μL (1 mL) with the concentration of the uptake solution maintained consistent with the original concentration of the target molecule mentioned previously in the article. Prior to the transition between solutions, the hydrogel was patted dry to ensure excess volume was removed; the weight was checked to ensure consistency with the original mass measurements, and the hydrogel was then introduced to the new solution. As the masses are fairly consistent, resembling a flat line, they are omitted from this study, as they do not provide sufficient context outside of a validation check.

Absorbance data from a spectrophotometer (the same used for UV−vis−NIR Analysis) was utilized to determine the concentration of the drug by invoking the Beer−Lambert Law which states that A is the absorbance, ε is the molar absorption coefficient, l is the path length, and c is the solution concentration. The accompanying formula states that the absorbance of the solution is directly proportional to the concentration, assuming that the molar absorption coefficient and path length remain constant throughout the experiment. The Beer−Lambert Law is stated below in eq 2,

$$A = \varepsilon l c \tag{2}$$

Prior to the utilization of this formula in experimentation, it was imperative to develop the standardization curve for the drug. Through varying the concentration of the drug between 0.001 and 0.10 mM at the peak signature of the drug, 295 nm, a standardization curve could be effectively developed as the concentration, molar absorption coefficient, and path length are known or remain constant in the experimentation. This experiment was conducted in both a phosphate buffer solution at pH 7.4 as well as DI water. The results can be found in Figure 2, below.

Through this standardization experiment, which takes the peak absorbance values at 295 nm for a variety of predeveloped concentrations of timolol maleate within either DI water or PBS solution, two independent linear equations can be gathered. The first equation, eq 3 expresses the concentration for the PBS solution which is the primary solution of consideration for future drug release experiments. The second, eq 4 is analyzed as well; however, it only serves as a check for the prior analysis of the released drug concentration.

https://doi.org/10.1021/acsomega.4c08540
ACS Omega 2025, 10, 4580−4587

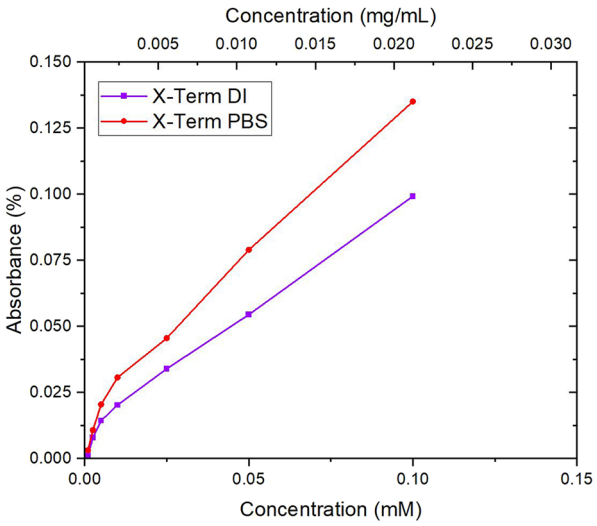

Figure 2. Target molecule calibration curve for timolol maleate which ranges in concentration between 0.001 mM (3.164×10^{-4} mg/mL) and 0.10 mM (0.03164 mg/mL). Solutions were prepared for both PBS and DI water solutions containing timolol maleate. The x-axis represents the absorbance expressed as a percentage, with the y-axes presenting the concentration in mg/mL (top) and mM (bottom), respectively.

$$y(x) = 4.0195x + 0.0112 \quad (3)$$

$$y(x) = 2.9563x + 0.0071 \quad (4)$$

Both equations exhibit linear behavior which is comparable to the Beer–Lambert Law of eq 2 which affirms the assumptions made previously of a constant path length and molar absorption coefficient. The y-terms of these equations represent the absorbance, while the x-terms of the equations represent the concentration of the drug in mg/mL. This experiment was repeated seven times with eqs 3 and 4 being developed as averages within 5% deviation of the maximum and minimum values collected. Thus, this model is statistically confident to be applied to further experimentation throughout this study.

3. RESULTS AND DISCUSSION

3.1. Hydrogel Sample Preparation. The prepared hydrogel samples can be broken down into two categories including molecular imprinted (MIP) and nonmolecular imprinted (NIP). Sufficient samples from each category were run (7 samples) to determine any statistical deviation or discontinuity, which will be described as necessary through the Results Section. As described in the Methods Section, the samples are poured into a mold, which is used to preserve the structure of the fluid until complete solidification. Figure 3, below, demonstrates the transition from pouring into the mold to the complete solidification of the hydrogel samples, ready for dimensioning, as described previously to maintain the normalization of sample sizes.

The samples, as prepared, are then cut down to 5×5 cm^2 squares as needed for future experimentation. Beyond this dimensional modification, however, no other modifications are made to the hydrogel samples during their experimentation to preserve the normalization standards to ensure cross-comparison between the individual samples regardless of their category (MIP or NIP) or sample number. This aids in further appreciation of all data sets for the prepared samples.

3.2. UV–Vis Transparency Analysis. As the prepared hydrogel samples are desired to be ocular drug delivery vehicles in the form of a contact lens, it is imperative to ensure that the transmission of light is not deterred in any way by the addition of drugs into the hydrogel matrix. Testing of the transmission was studied on both MIP and NMIP samples to better understand the optical differences between the two target molecule incorporation mechanisms. The results of this experimentation are demonstrated in Figure 4.

An investigation of the prepared hydrogel samples between the wavelengths of 300–1000 nm demonstrates the optical performance of these samples, asserting that due to the near or above 90% transmittance value, they can be successfully implemented as a contact lens-based drug delivery vehicle. The NIP hydrogel samples have much worse optical performance than their MIP counterparts, hinting at a possible boundary layer of water or unbound target molecule, occluding the hydrogel from effectively transmitting light through.

3.3. FT-IR Structural Analysis. FT-IR is an invaluable tool for determining the chemical structure nature of the prepared samples, especially hydrogel samples. This tool can be jointly used to determine the overall chemical structure of the prepared samples in addition to providing insight into the target molecule incorporation into the hydrogel matrix. The chemical structure is visualized in Figure 5, below, through the

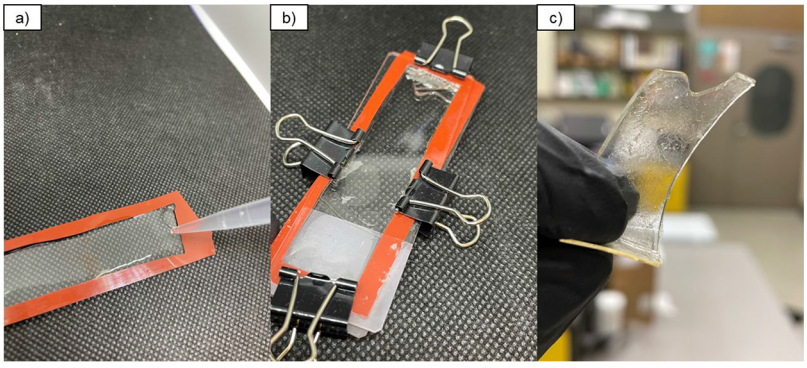

Figure 3. (a) Pouring is done into a mold, which seeks to preserve the structure of the samples until solidified. (b) After mixing and pouring, samples are retained in a mold to preserve their structure until solidified. This mold is joined together through binder clips to ensure that no fluid escapes from the mold vessel. (c) Final samples as prepared, prior to redimensioning required for the individual experiments as described in the Methods Section of this article.

https://doi.org/10.1021/acsomega.4c08540
ACS Omega 2025, 10, 4580–4587

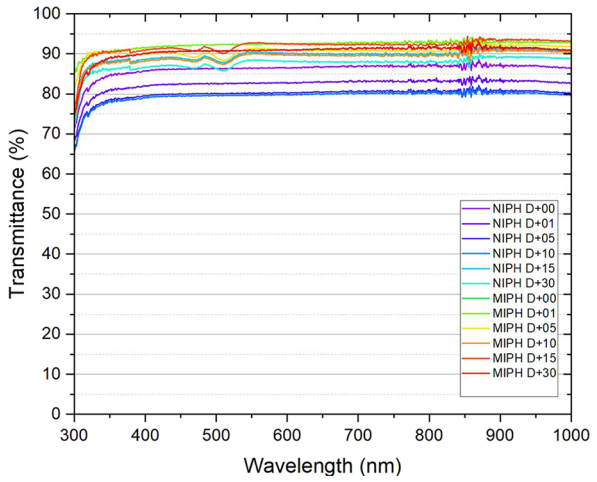

Figure 4. UV−vis−NIR spectra for the two categories of MIPH and NIPH hydrogel samples studied. The *y*-axis is the transmittance in a percentage expressed as a function of the *x*-axis, wavelength in units of nm.

appearance of functional groups which present themselves as absorption bands in a spectrum.

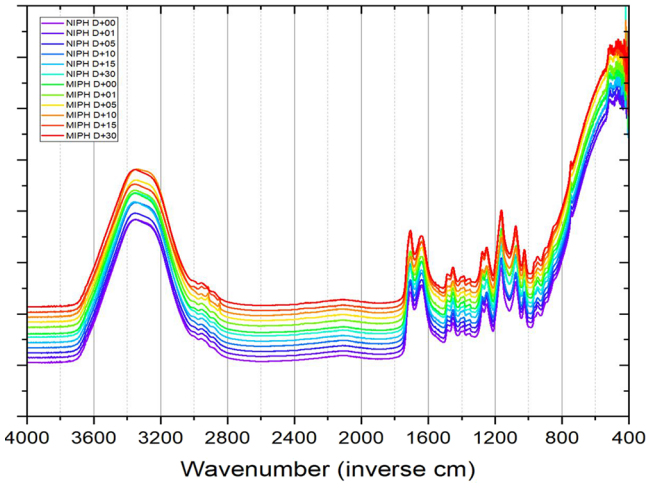

Figure 5. FT-IR spectra for the two categories of MIPH and NIPH hydrogel samples studied. The *y*-axis is left in terms of arbitrary units however is functionally the transmittance (%) allowing for the visualization of discrete peaks while the *x*-axis demonstrates the wavenumber in units of inverse cm.

FT-IR demonstrates the chemical structure of prepared hydrogel samples between the wavenumber of 4000−400 nm whereby this range remains consistent across all NIP and MIP samples. The analysis was conducted to verify the end-state composition aligned with the input formulation and the literature-acceptable functional groups for methacrylate-based polymers and, in particular, hydrogels of this chemistry. Functional groups identified from the FT-IR spectra include alkene (C═C), amine (C−N), ether (C−O−C), and alkane (C−H) which correspond to peak signatures at 1505, 1317, 1250, and 660 wavenumbers, respectively. The spectra collected demonstrate consistency between the NIP and MIP samples and maintenance in the spectra at 30 days of testing, indicating that there are no sizable chemical changes or deviations in the structure which could be correlated to a depreciation in the drug release or swelling kinetics. This spectra analysis serves as a check for the information beyond this piece asserting that no chemical fluctuations are present, which would describe the deviations present in the swelling kinetics, drug uptake and release kinetics, and overall longevity studies of the hydrogel samples presented in this article.

3.4. Swelling Kinetics. The swelling kinetics expressed as the swelling ratio in grams/g throughout the period of 30 days was analyzed for both the MIPH and NIPH samples presented in this article to determine what, if any, deviations in the swelling ratio occur between these regimes and their progression throughout a time period of 30 days. This was conducted by motivating the use of eq 2 whereby the mass could be measured at each timestamp and subsequently, the swelling ratio could be determined as the initial dry mass is a known quantity. As can be visualized, NIPH samples are more prone to swelling than their MIPH counterparts, contributing to a maximum measured swelling ratio of 1.773 g/g at Day 0 which decreases rather gradually to a maximum measured swelling ratio of 1.512 g/g at Day 30 which concludes the testing. Likewise, the MIPH samples demonstrate a gradual decrease from a maximum measured swelling ratio of 1.476 g/g on Day 0 to 1.403 g/g on Day 30. Given the nature of the decrease over the 30 days of testing, it can be determined that MIPH offers more stability in part due to the smaller pore size due to the drug loading within the matrix. This allows for the hydrogel to maintain its rigidity much more than the NIPH which suffers from an increased pore size, which translates into both a faster decrease from the maximum measured swelling ratio as well as the nature of the decrease in over 0.2 g/g, which is much greater than the 0.07 g/g decrease of the MIPH samples tested. Figure 6, below, demonstrates the change in the swelling ratio throughout the duration of the experiment.

The swelling kinetics for the tested samples, as visualized by Figure 5, demonstrate the differences in the porosity between the MIPH and NIPH samples due to the incorporation of drug into the hydrogel matrix in the case of the MIPH which is attributed to differences in the maximum measured swelling ratios over the testing period of 30 days. Particularly, the use of

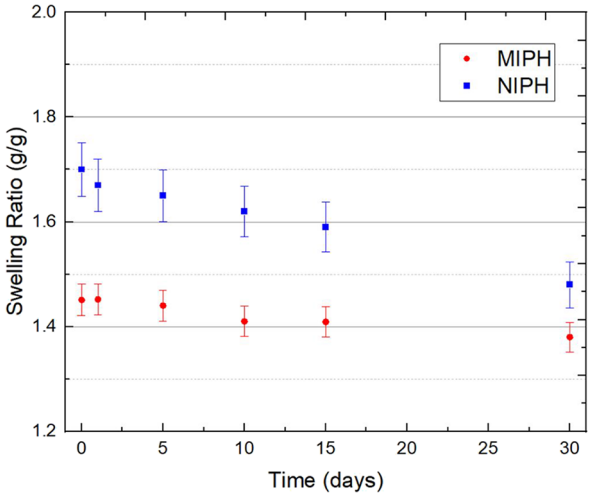

Figure 6. Swelling kinetics for the two categories MIPH and NIPH hydrogel samples studied. The *y*-axis here demonstrates the swelling ratio in g/g ranging from 1.2 to 2.0 while the *x*-axis provides the period of testing ranging from 0 to 30 days. Measurements were taken at 0 days, 1 days, 5 days, 10 days, 15 days, and 30 days.

https://doi.org/10.1021/acsomega.4c08540
ACS Omega 2025, 10, 4580−4587

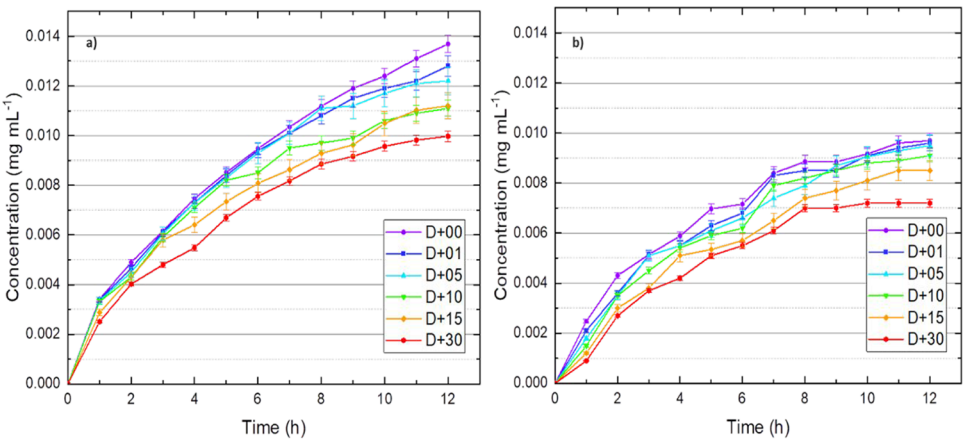

Figure 7. Drug release concentration for the two categories (a) MIPH and (b) NIPH of hydrogel samples studied. The *y*-axis demonstrates the concentration in mg/mL ranging from 0 to 0.014, while the *x*-axis provides the release sampling period from 0 to 12 h. Measurements were taken at 0 days, 1 days, 5 days, 10 days, 15 days, and 30 days as indicated by the "D+##" legend.

imprinting corresponds to an enhanced matrix stability which allows consistency in the swelling kinetics over the course of the period as noticed through the differences in the relative decreases of the maximum measured swelling ratio between the MIPH and NIPH samples.

3.5. Drug Uptake and Release Kinetics. As a primary curiosity of the investigation related to hydrogel samples as probable drug delivery vehicles, the drug uptake and release kinetics were analyzed across a 30-day sampling period for both MIPH and NIPH samples. During this period, hydrogels were immersed in solutions, either the release or uptake solution for 12 h each. The release solution contains PBS while the uptake solution contains the original concentration of the target molecule. Through motivating eq 2, the Beer–Lambert Law, the absorbance could be equated to the concentration of the target molecule found in the solution, and subsequently, knowing the standard for timolol maleate in eqs 3 and 4, a reliable concentration of target molecule could be determined for this experiment. Each category of sample was tested for a 12 h time frame as consistent with our prior methodology. Each run was completed using independent samples in a series of seven (7) to establish a statistical baseline for any observations collected. Using Beer–Lambert Law, the concentration of the drug released was determined from UV–vis–NIR spectra as per eq 3 earlier in this article. Figures 7 and 8 seek to map the drug uptake and release kinetics within both a 12 h period as well as the changes in these values over a sampling time period of 30 days to determine what, if any, changes occur in the release profile and kinetics over time. Deviations in the release kinetics are considerably undesirable for the implementation of these materials as controlled and sustained drug release vehicles capable of performing drug delivery throughout the duration of a typical contact lens use.

As demonstrated by the graphs above, MIPH performance is quite discernible from NIPH, offering heightened releasable concentration from the hydrogel matrix. Throughout the 30-day trial, the concentration of MIP maintained well above 0.009 mg/mL for the duration of testing, while the NIPH failed to exceed 0.009 mg/mL even on the first day of testing in this experiment. On Day 1 respectively, the MIPH maintains a releasable concentration of 0.0138 mg/mL (±0.002 mg/mL) which undergoes a decrease to approximately 0.0112 mg/mL (±0.0013 mg/mL) at Day 30 of experimentation. Comparably

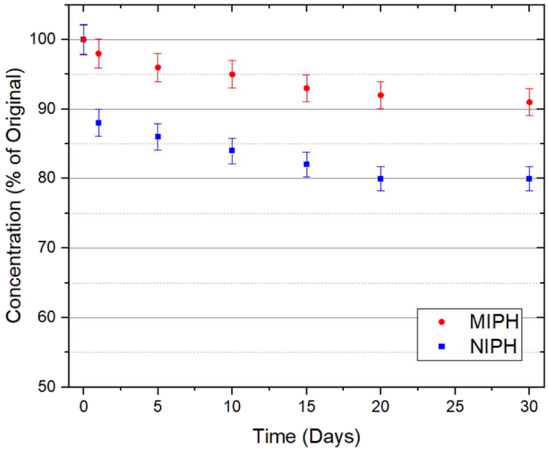

Figure 8. Lifetime kinetics for the two categories of MIPH and NIPH hydrogel samples studied. The *y*-axis demonstrates the concentration expressed as a percentage of the original value (as the original value is known) ranging from 50% to 100% providing the period of testing ranging from 0 to 30 days. Measurements were taken at 0 days, 1 days, 5 days, 10 days, 15 days, and 30 days.

this is a lesser decrease and more stabilized performance over time compared to NIPH samples which undergo a change in the releasable concentration of 0.00093 mg/mL (±0.00015 mg/mL) at Day 1 to 0.00065 mg/mL (±0.00009 mg/mL) at Day 30. While the decrease in the NIPH is considerably less than that of the MIPH samples in terms of the raw number, the depreciation in the concentration capability is much greater in comparison corresponding to a 19.92% decrease in the MIPH and a 30.11% decrease in the NIPH. Effectively this means that while the release kinetics of the MIPH are depreciated by a fifth in the MIPH, nearly a third of the capable release in NIPH is depreciated over the same period.

Building upon this information, the lifetime kinetics for each sample and MIPH and NIPH were measured over the 30-day time period with measurement increments at 0 days, 1 days, 5 days, 10 days, 15 days, and 30 days in line with other experimentation presented in this article. This data is used in conjunction with the previous drug release kinetics data to explore more precisely the depreciation of the drug release capability over the 30-day measurement period.

https://doi.org/10.1021/acsomega.4c08540
ACS Omega 2025, 10, 4580–4587

Namely, a similar trend between the MIPH and NIPH hydrogel samples was determined where the NIPH exhibits a much more varied decrease initially with a final stabilization in the values, while the MIPH samples exhibit a more controlled decrease initially and a gradual decreasing stabilization in values. Numerically, this corresponds to a final change in the releasable concentration of 92.45% (±1.15%) for the MIPH samples and 80.03% (±1.01%) in the NIPH samples respectively. Broadly this means that while both samples exhibit decreases in their loadable concentration from Day 0 to Day 30, MIPH samples are more capable in their ability to absorb and desorb amounts of drug solution due to the incorporation of recognition sites in the hydrogel matrix which are not present in the NIPH samples; thus, the MIPH samples provide a more controlled and sustained interaction at the matrix-level compared to NIPH samples.

4. CONCLUSIONS

Hydrogels are of notable research interest in the context of biomedical materials, especially in drug delivery applications due to their capability to have a tunable and determinable stimuli-response, maintain biocompatibility, and absorb and desorb vast quantities of water without destruction of the matrix. Through investigation of the spectroscopic, chemical, swelling, and drug kinetics properties of a HEMA hydrogel system, determinations could be inferred regarding the importance of incorporating recognition sites into the hydrogel that are necessary to ensure a controlled and sustained drug interaction. Hydrogels with imprinting (MIPH) demonstrated a more stable drug release profile than nonimprinted (NIPH) counterparts throughout a month of testing. During this testing, as well, it was determined that recognition sites incorporated into the hydrogel matrix allow for release over the course of a month of testing. In addition, MIPH demonstrates a more controlled swelling response to external stimuli, balancing this swelling nature while limiting changes in dimensionality which may be cause for concern when applying these materials as ocular drug delivery systems where extensive swelling may cause unnecessary side effects such as irritation. Through the evidenced spectroscopic data, there are no chemical or structural changes in the material, and thus, the determination can be accurately suggested that MIPH, through its recognition capacity alone, is an amble selection in terms of the swelling response, drug release kinetics, and the longevity of performance of these hydrogels.

■ ASSOCIATED CONTENT

Data Availability Statement

Data will be made available upon a reasonable request.

■ AUTHOR INFORMATION

Corresponding Author

Jeffrey S. Bates − *Department of Materials Science and Engineering, University of Utah, Salt Lake City, Utah 84112, United States*; Email: jeff.bates@utah.edu

Author

Parker M. Toews − *Department of Materials Science and Engineering, University of Utah, Salt Lake City, Utah 84112, United States*; orcid.org/0000-0002-0338-018X

Complete contact information is available at: https://pubs.acs.org/10.1021/acsomega.4c08540

Author Contributions

Data curation, P.T.; investigation, P.T.; methodology, P.T.; project administration, J.B.; writing-original draft, P.T., writing-review and editing, P.T. and J.B.; All authors have read through and agree to the published version of the manuscript.

Notes

The authors declare no competing financial interest.

■ ACKNOWLEDGMENTS

FT-IR and UV−vis−NIR measurements were performed at the University of Utah's Materials Characterization Lab.

■ REFERENCES

(1) Hsu, E.; Desai, M. Glaucoma and Systemic Disease. *Life* **2023**, *13* (4), 1018.

(2) Tseng, S. C. Evaluation of the Ocular Surface in Dry-Eye Conditions. *International ophthalmology clinics* **1994**, *34* (1), 57−69.

(3) Akpek, E. K.; Smith, R. A. Overview of Age-Related Ocular Conditions. *Am. J. Manage. Care* **2013**, *19*, S67−S75.

(4) Papas, E. B. The Global Prevalence of Dry Eye Disease: A Bayesian View. *Ophthalmic Physiol Opt* **2021**, *41* (6), 1254−1266.

(5) Oliver, J. E.; Hattenhauer, M. G.; Herman, D.; Hodge, D. O.; Kennedy, R.; Fang-Yen, M.; Johnson, D. H. Blindness and Glaucoma: A Comparison of Patients Progressing to Blindness from Glaucoma with Patients Maintaining Vision. *American journal of ophthalmology* **2002**, *133* (6), 764−772.

(6) Marshall, L. L.; Roach, J. M. Treatment of Dry Eye Disease. *Consult. Pharm.* **2016**, *31* (2), 96−106.

(7) Quaranta, L.; Novella, A.; Tettamanti, M.; Pasina, L.; Weinreb, R. N.; Nobili, A. Adherence and Persistence to Medical Therapy in Glaucoma: An Overview. *Ophthalmol. Ther.* **2023**, *12*, 2227−2240.

(8) McDonald, H. P.; Garg, A. X.; Haynes, R. B. Interventions to Enhance Patient Adherence to Medication Prescriptions: Scientific Review. *Jama* **2002**, *288* (22), 2868−2879.

(9) Sleath, B.; Blalock, S.; Covert, D.; Stone, J. L.; Skinner, A. C.; Muir, K.; Robin, A. L. The Relationship between Glaucoma Medication Adherence, Eye Drop Technique, and Visual Field Defect Severity. *Ophthalmology* **2011**, *118* (12), 2398−2402.

(10) Biran, A.; Goldberg, M.; Shemesh, N.; Achiron, A. Improving Compliance with Medical Treatment Using Eye Drop Aids. *Encyclopedia* **2023**, *3* (3), 919−927.

(11) Cope, J.; Collier, S.; Rao, M.; Chalmers, R.; Mitchell, G.; Richdale, K.; Wagner, H.; Kinoshita, B.; Lam, D.; Faao, L.; Zimmerman, A.; Yoder, J.; Beach, M. Contact Lens Wearer Demographics and Risk Behaviors for Contact Lens-Related Eye Infections - United States, 2014. *MMWR Morb. Mortal Wkly. Rep.* **2015**, *64*, 865−870.

(12) Key, J. E. Development of Contact Lenses and Their Worldwide Use. *Eye Contact Lens* **2007**, *33* (6Pt 2), 343−345.

(13) Fischer, L.; Mueller, R.; Ekberg, B.; Mosbach, K. Direct Enantioseparation of.Beta.-Adrenergic Blockers Using a Chiral Stationary Phase Prepared by Molecular Imprinting. *J. Am. Chem. Soc.* **1991**, *113* (24), 9358−9360.

(14) Uchino, M.; Yokoi, N.; Shimazaki, J.; Hori, Y.; Tsubota, K.; Society, O. B. O. T. J. D. E. Adherence to Eye Drops Usage in Dry Eye Patients and Reasons for Non-Compliance: A Web-Based Survey. *J. Clin Med.* **2022**, *11* (2), 367.

(15) Heller, J.; Peppas, N. A. *Hydrogels in Medicine and Pharmacy*, 1987; Vol. 3.

(16) Liu, Y.; Wang, L.; Mi, Y.; Zhao, S.; Qi, S.; Sun, M.; Peng, B.; Xu, Q.; Niu, Y.; Zhou, Y. Transparent Stretchable Hydrogel Sensors: Materials, Design and Applications. *Journal of Materials Chemistry C* **2022**, *10* (37), 13351−13371.

(17) Ko, J.; Kim, C.; Kim, D.; Song, Y.; Lee, S.; Yeom, B.; Huh, J.; Han, S.; Kang, D.; Koh, J.-S.; et al. High-Performance Electrified Hydrogel Actuators Based on Wrinkled Nanomembrane Electrodes

https://doi.org/10.1021/acsomega.4c08540
ACS Omega 2025, 10, 4580−4587

for Untethered Insect-Scale Soft Aquabots. *Sci. Rob.* **2022**, *7* (71), No. eabo6463.
(18) Radulescu, D.-M.; Neacsu, I. A.; Grumezescu, A.-M.; Andronescu, E. New Insights of Scaffolds Based on Hydrogels in Tissue Engineering. *Polymers* **2022**, *14* (4), 799.
(19) Andrews, P.; Craik, D.; Martin, J. Functional Group Contributions to Drug-Receptor Interactions. *Journal of medicinal chemistry* **1984**, *27* (12), 1648−1657.
(20) Hoque, M.; Alam, M.; Wang, S.; Zaman, J. U.; Rahman, M. S.; Johir, M.; Tian, L.; Choi, J.-G.; Ahmed, M. B.; Yoon, M.-H. Interaction Chemistry of Functional Groups for Natural Biopolymer-Based Hydrogel Design. *Materials Science and Engineering: R: Reports* **2023**, *156*, No. 100758.
(21) Adler, G. Cross-Linking of Polymers by Radiation. *Science* **1963**, *141* (3578), 321−329.
(22) Maitra, J.; Shukla, V. Cross-Linking in Hydrogels − A Review. *Am. J. Polym. Sci.* **2014**, *4*, 25−31.
(23) Hennink, W. E.; van Nostrum, C. F. Novel Crosslinking Methods to Design Hydrogels. *Adv. Drug Delivery Rev.* **2012**, *64*, 223−236.
(24) Bordbar-Khiabani, A.; Gasik, M. Smart Hydrogels for Advanced Drug Delivery Systems. *International Journal of Molecular Sciences* **2022**, *23* (7), 3665.
(25) Ho, T.-C.; Chang, C.-C.; Chan, H.-P.; Chung, T.-W.; Shu, C.-W.; Chuang, K.-P.; Duh, T.-H.; Yang, M.-H.; Tyan, Y.-C. Hydrogels: Properties and Applications in Biomedicine. *Molecules* **2022**, *27* (9), 2902.
(26) Tokarev, I.; Minko, S. Stimuli-Responsive Hydrogel Thin Films. *Soft Matter* **2009**, *5* (3), 511−524.
(27) Brighenti, R.; Cosma, M. P. Mechanics of Multi-Stimuli Temperature-Responsive Hydrogels. *Journal of the Mechanics and Physics of Solids* **2022**, *169*, No. 105045.
(28) Anderson, J. M. Biological Responses to Materials. *Annu. Rev. Mater. Res.* **2001**, *31* (1), 81−110.
(29) Chen, Y.; Liu, T.; Wang, G.; Liu, J.; Zhao, L.; Yu, Y. Highly Swelling, Tough Intelligent Self-Healing Hydrogel with Body Temperature-Response. *Eur. Polym. J.* **2020**, *140*, No. 110047.
(30) Hiratani, H.; Fujiwara, A.; Tamiya, Y.; Mizutani, Y.; Alvarez-Lorenzo, C. Ocular Release of Timolol from Molecularly Imprinted Soft Contact Lenses. *Biomaterials* **2005**, *26* (11), 1293−1298.
(31) Bodoki, A. E.; Iacob, B.-C.; Dinte, E.; Vostinaru, O.; Samoila, O.; Bodoki, E. Perspectives of Molecularly Imprinted Polymer-Based Drug Delivery Systems in Ocular Therapy. *Polymers* **2021**, *13* (21), 3649.
(32) Amna, R.; Ali, K. Molecularly Imprinted Hydrogel Sensor for Proteins. *J. Dispersion Sci. Technol.* **2023**, *45*, 1086−1095.
(33) Hu, X.; Vatankhah-Varnoosfaderani, M.; Zhou, J.; Li, Q.; Sheiko, S. S. Weak Hydrogen Bonding Enables Hard, Strong, Tough, and Elastic Hydrogels. *Advanced materials* **2015**, *27* (43), 6899−6905.
(34) Peppas, N. A.; Mikos, A. G. Preparation Methods and Structure of Hydrogels. In *Hydrogels in medicine and pharmacy*; CRC press, 2019; pp 1−26.
(35) Palantöken, S.; Bethke, K.; Zivanovic, V.; Kalinka, G.; Kneipp, J.; Rademann, K. Cellulose Hydrogels Physically Crosslinked by Glycine: Synthesis, Characterization, Thermal and Mechanical Properties. *J. Appl. Polym. Sci.* **2020**, *137* (7), 48380.
(36) Zhang, C.; Zhou, Y.; Han, H.; Zheng, H.; Xu, W.; Wang, Z. Dopamine-Triggered Hydrogels with High Transparency, Self-Adhesion, and Thermoresponse as Skinlike Sensors. *ACS Nano* **2021**, *15* (1), 1785−1794.
(37) Li, H.; Liu, Y.; He, X.; Ding, Y.; Yan, H.; Xie, P.; Yang, W. Electrospinning technology in tissue engineering scaffolds. *Sheng Wu Gong Cheng Xue Bao* **2012**, *28* (1), 15−25.
(38) Bayer, I. S. Controlled Drug Release from Nanoengineered Polysaccharides. *Pharmaceutics* **2023**, *15* (5), 1364.
(39) Toews, P.; Bates, J. Influence of Drug and Polymer Molecular Weight on Release Kinetics from HEMA and HPMA Hydrogels. *Sci. Rep.* **2023**, *13* (1), 16685.
(40) Ramkissoon-Ganorkar, C.; Liu, F.; Baudys, M.; Kim, S. W. Effect of Molecular Weight and Polydispersity on Kinetics of Dissolution and Release from Ph/Temperature-Sensitive Polymers. *J. Biomater. Sci., Polym. Ed.* **1999**, *10* (10), 1149−1161.
(41) Abdi, B.; Mofidfar, M.; Hassanpour, F.; Cilingir, E. K.; Kalajahi, S. K.; Milani, P. H.; Ghanbarzadeh, M.; Fadel, D.; Barnett, M.; Ta, C. N. Therapeutic Contact Lenses for the Treatment of Corneal and Ocular Surface Diseases: Advances in Extended and Targeted Drug Delivery. *Int. J. Pharm.* **2023**, *638*, No. 122740.

https://doi.org/10.1021/acsomega.4c08540
ACS Omega 2025, 10, 4580−4587